FORMATION OF THE BLACK HOLE IN NOVA SCORPII

PHILIPP PODSIADLOWSKI
Oxford University, Oxford, OX1 3RH, UK; podsi@astro.ox.ac.uk

KEN'ICHI NOMOTO
Department of Astronomy and Research Center for the Early Universe, School of Science, University of Tokyo, Bunkyo-ku, Tokyo 113-0033, Japan; nomoto@astron.s.u-tokyo.ac.jp

KEIICHI MAEDA
Department of Astronomy, School of Science, University of Tokyo, Bunkyo-ku, Tokyo 113-0033, Japan; maeda@astron.s.u-tokyo.ac.jp

TAKAYOSHI NAKAMURA
Department of Astronomy, School of Science, University of Tokyo, Bunkyo-ku, Tokyo 113-0033, Japan; nakamura@astron.s.u-tokyo.ac.jp

PAOLO MAZZALI
Osservatorio Astronomico di Trieste, Via G. B. Tiepolo 11, I-34131 Trieste, Italy; and Research Center for the Early Universe, School of Science, University of Tokyo, Tokyo 113-0033, Japan; mazzali@ts.astro.it

AND

BRIAN SCHMIDT
Research School of Astronomy and Astrophysics, Australian National University, Weston Creek, ACT 2611, Australia; brian@mso.anu.edu.au
Received 2001 April 20; accepted 2001 November 1

ABSTRACT

Israelian and coworkers showed that the stellar companion of the black hole binary Nova Sco is polluted with material ejected in the supernova that accompanied the formation of the black hole primary. Here we systematically investigate the implications of these observations for the black hole formation process. Using a variety of supernova models, including standard as well as hypernova models (for different helium star masses, explosion energies, and explosion geometries) and a simple model for the evolution of the binary and the pollution of the secondary, we show that most of the observed abundance anomalies can be explained for a large range of model parameters (apart from the abundance of Ti). The best models are obtained for He star masses of 10–16 $M_\odot$, where spherical hypernova models are generally favored over standard supernova ones. Aspherical hypernova models also produce acceptable fits, provided there is extensive lateral mixing. All models require substantial fallback and that the fallback material either reached the orbit of the secondary or was mixed efficiently with material that escaped. The black hole therefore formed in a two-step process, where the initial mass of the collapsed remnant was increased substantially by matter that fell back after the initial collapse. This may help to explain the high observed space velocity of Nova Sco either because of a neutrino-induced kick (if a neutron star was formed first) or by asymmetric mass ejection in an asymmetric supernova explosion.

Subject headings: binaries: close — black hole physics — stars: evolution
— stars: individual (Nova Scorpii 1994) — supernovae: general — X-rays: binaries

1. INTRODUCTION

X-ray Nova Scorpii 1994 (GRO J1655−40; hereafter Nova Sco) is one of the best-studied black hole transients of recent years (e.g., Bailyn et al. 1995; Harmon et al. 1995; Hjellming & Rupen 1995; Tingay et al. 1995; Orosz & Bailyn 1997; van der Hooft et al. 1998; Shahbaz et al. 1999). It is a low-mass black hole binary with an orbital period of 2.61 days and relatively well-determined component masses. The most recent and most self-consistent analysis of the ellipsoidal light curves of the system by Beer & Podsiadlowski (2002) has yielded masses of 5.4 ± 0.3 and 1.45 ± 0.35 $M_\odot$ for the black hole and the secondary, respectively, which we adopt in this study.[1]

Nova Sco stands out among the black hole transients

[1] The studies by Orosz & Bailyn (1997) and van der Hooft et al. (1998) obtained somewhat higher masses for both components. However, both of these studies used a color excess, $E(B-V) \simeq 1.3$, that is too large to be consistent with the observed colors of the secondary in Nova Sco, assuming that its spectral type is in the range of F2–F7 III/IV (see Beer & Podsiadlowski 2002 for details).

because of an unusually high space velocity. Using the γ-velocity of Shahbaz et al. (1999) and the corrections for Galactic rotation of Brandt, Podsiadlowski, & Sigurdsson (1995), Nova Sco's space velocity must exceed 106 km s^{-1}, a factor of a few larger than in any other low-mass black hole transient. Brandt et al. (1995) concluded that the most likely explanation for the high space velocity is that the black hole formed in a two-stage process where the initial collapse led to the formation of a neutron star accompanied by a substantial kick (Lyne & Lorimer 1994). The neutron star was subsequently converted into a black hole by accretion of matter that was not ejected in the supernova or a phase transition in the cooling compact object (Brown & Bethe 1994). (See also Fryer & Kalogera 2001 and, for a different view, Nelemans, Tauris, & van den Heuvel 1999.)

That the black hole formed in a supernova event was confirmed by Israelian et al. (1999). Using high-resolution echelle spectroscopy with the Keck Telescope, they showed that the atmosphere of the secondary was enriched by a factor of 6–10 in several α-process elements (O, Mg, Si, S,

TABLE 1

Observed Abundances in the Secondary of Nova Sco

Parameter	N	O	Mg	Si	S	Ti	Fe
$[X_i/H]$	0.45	1.00	0.90	0.90	0.75	0.90	0.10
$\Delta[X_i/H]$	0.50	0.30	0.40	0.30	0.20	0.40	0.20

Note.—$[X_i/H]$: logarithmic abundances relative to solar; $\Delta[X_i/H]$: observational uncertainties in $[X_i/H]$. From Israelian et al. 1999.

and Ti; see Table 1). Since some of these elements are almost exclusively synthesized during a supernova explosion and cannot have been produced in a low-mass secondary, the secondary must somehow have been exposed to supernova material that was ejected when the compact object in Nova Sco was formed. It should be noted that it is by no means required that the formation of a black hole is accompanied by a supernova-like event. If a black hole forms promptly, i.e., on the dynamical timescale of the collapsing core, very few neutrinos can escape from the collapsing object (e.g., Gourgoulhon & Haensel 1993). Since delayed neutrino heating may be an essential feature in producing a successful ejection of the stellar envelope, i.e., a supernova, a lack of neutrino emission may lead to a "failed" supernova in which the whole star collapses into a black hole. In this case, no pollution of the secondary is expected, neither is a supernova kick. The observations of Israelian et al. (1999) immediately rule out a simple prompt black hole formation scenario for Nova Sco without an accompanying supernova and suggest that the black hole formed in a two-step process, where a neutron star may have formed first and was subsequently converted into a black hole by accretion. Alternatively, a black hole may have formed promptly, but subsequent accretion from a surrounding disk could have driven a jetlike explosion, as in the collapsar models of MacFadyen & Woosley (1999). In either case, the compact star could have received a substantial kick, in the first case due to an asymmetry in the neutrino emission (as may be the cause of neutron star kicks), in the latter perhaps because of an asymmetry in the jets.

The purpose of the present study is to explore the implications of the observations of Israelian et al. (1999) for the formation of the black hole in Nova Sco in some detail. While Si is enriched by a factor of 8, Fe—surprisingly—is not. Since both of these elements are produced close to the mass cut above which matter is ejected in a successful supernova, these observations directly probe the region that is most crucial in determining whether a supernova is successful or fails. Indeed, the observations pose an immediate problem, since, in a standard supernova, the mass cut ($M_{\rm cut} \simeq 1.5$–2 $M_\odot$; Thielemann, Nomoto, & Hashimoto 1996) is much smaller than the present mass of the black hole in Nova Sco. Figure 1a shows the composition of the ejecta for a 16 $M_\odot$ helium star for a standard supernova (i.e., with a canonical explosion energy $E_K = 1 \times 10^{51}$ ergs; from Nakamura et al. 2001). Elements such as S and Si, both enhanced significantly in the companion of Nova Sco, are produced between the innermost 2.5 and 3.5 $M_\odot$ of the helium core, well below the final mass of the black hole. There are four possible ways by which some matter synthesized in this region can reach the secondary and by which the mass of the black hole can be increased to the present value: (1) by fallback of material in the supernova explosion (Woosley & Weaver 1995), (2) by postsupernova mass transfer from the secondary, (3) as a result of mixing during the collapse phase, and (4) as a result of a more energetic supernova (a hypernova with a larger mass cut). The composition of a hypernova model (with $E_K = 3 \times 10^{52}$ ergs) is shown in Figure 1b. It illustrates how, for a more energetic hypernova, elements such as S and Si are produced much farther out in the core of the helium star. Indeed, it was this model that motivated Israelian et al. (1999) to first suggest a hypernova model for the formation of the black hole in Nova Sco. This and a possible connection to gamma-ray
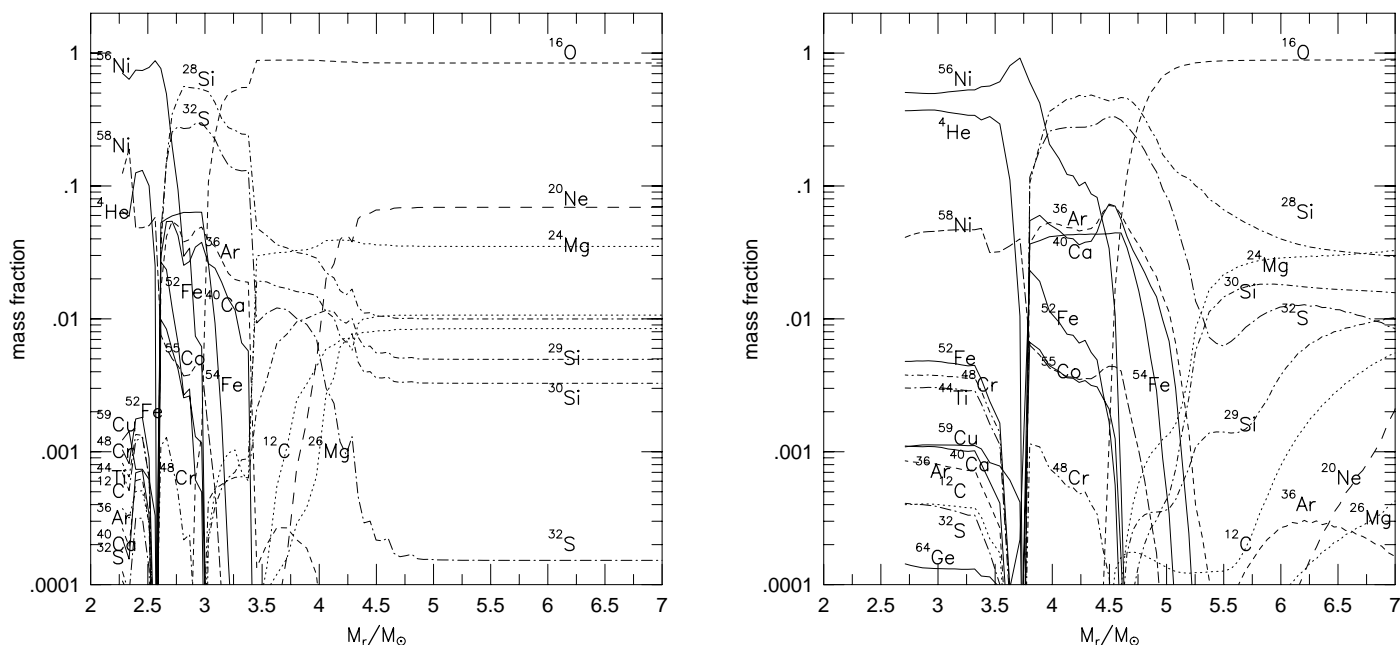

Fig. 1.—Isotopic chemical composition for a 16 $M_\odot$ He star for (a) a normal supernova with explosion energy $E_K = 1 \times 10^{51}$ ergs and (b) a hypernova with explosion energy $E_K = 3 \times 10^{52}$ ergs (from Nakamura et al. 2001).

bursts was further developed by Brown et al. (2000). These various solutions are, of course, not mutually exclusive, and we shall consider all of them in the following sections (see Fig. 2 for a schematic picture of the various cases considered).

2. MODELING THE POLLUTION IN THE SECONDARY

In order to examine whether the observed pollution of the secondary is consistent with the predictions of stellar and supernova nucleosynthesis, we have to follow the evol-

ution of the binary through various evolutionary phases before and after the supernova and need to model the pollution of the secondary. In this section we present a very simple model that includes the main physical effects. Its purpose is to serve as a reference model with which we can discuss the physical implications of the observed abundance anomalies. In § 3 we critically assess some of the assumptions in this model and successively add physical realism to the model by first including mixing in the ejecta (§§ 3.3 and 3.4) and then considering an aspherical explosion (§ 3.5).

1. Wide binary with massive primary star and intermediate-mass companion.

2. Spiral-in of secondary in red supergiant phase leads to ejection of the hydrogen-rich envelope and produces short-period helium star binary.

Case A
Case B
Case C

3ab. Core collapse creates neutron star and leads to ejection of primary's envelope.

Case A

4a. Fallback of debris, some of which has passed the secondary, commences.

5ab. Expanding debris deposits synthesized elements on secondary. Fallback creates black hole.

Case B

4b. Fallback occurs in region interior to secondary's orbit, with significant mixing of the material at the fallback interface.

Case C

3c. Asymmetric core collapse creates neutron star/black hole and initiates aspherical expansion of the primary's envelope.

4c. Mixing occurs on the fallback interface. The material in the equatorial region expands more slowly than along the poles.

5c. Fallback increases mass of compact object. Slow-moving equatorial debris deposits synthesized material on secondary.
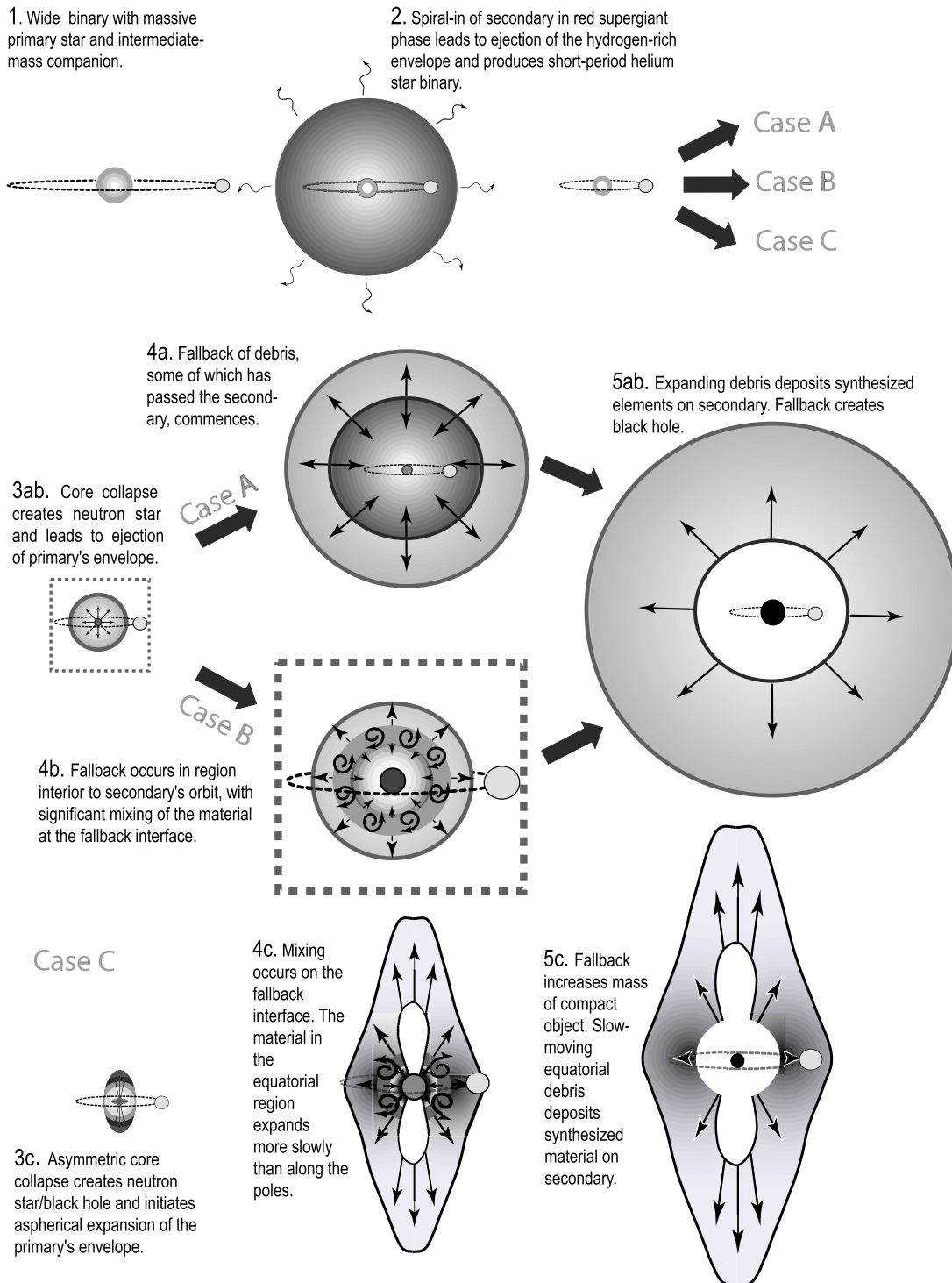
FIG. 2.—Schematic diagram for the various pollution scenarios considered

As the model becomes more realistic, the modeling uncertainties also increase.

2.1. Description of the Model without Mixing (Case A)

The calculation of the pollution of the secondary requires stellar models that have been subjected to explosive nuclear burning in a supernova event. We take these from the library of models calculated by Nomoto et al. (1997, 2001a, 2001b). At the time of the explosion, the immediate supernova progenitor had to be a helium star (or Wolf-Rayet star) in order to fit into the tight binary orbit implied by the present orbital period of Nova Sco. We consider helium stars with initial helium star masses, $M_{\rm He}^0$, of 6, 8, 10, and 16 $M_\odot$. These correspond to main-sequence masses of ~ 20, 25, 30, and 40 $M_\odot$, respectively. We consider two classes of explosion models: supernova models that have a standard supernova explosion energy of 1 foe (1 foe $\equiv 10^{51}$ ergs) and hypernova models with explosion energies of 8 and 30 foe (for the 10 $M_\odot$ model) and 30 foe (for the 16 $M_\odot$ model). The 6 $M_\odot$ model is a model calculated for SN 1987A, while the 30 foe, 16 $M_\odot$ model is appropriate for the prototype hypernova SN 1998bw (Iwamoto et al. 1998; Nakamura et al. 2001).[2]

Helium/Wolf-Rayet stars are known to lose a substantial fraction of their envelopes in a stellar wind. To take this into account, we assume that the helium star has lost an amount $\Delta M_{\rm He} = g(M_{\rm He}^0 - M_{\rm BH}^0)$ before the explosion, where $M_{\rm BH}^0$ is the initial mass of the compact remnant (neutron star or black hole). We use the parameter g to vary the total amount of wind mass loss before the supernova.

At the time of the explosion, the masses of the primary and secondary are $M_{\rm He}$ and M_2^0, respectively. When the primary collapses, it first forms a compact remnant of mass $M_{\rm BH}^0$. The rest of the envelope is assumed to be ejected initially, but part of it ($M_{\rm fallback}$) will subsequently fall back, either because it did not achieve escape velocity or because it was pushed back by a reverse shock in the envelope (see Woosley & Weaver 1995). The fallback matter increases the mass of the compact remnant to $M_{\rm BH}^1$ (indeed, it may be this fallback that leads to the conversion of the compact remnant into a black hole). Figure 3a schematically illustrates the definition of these various mass parameters.

In the simple model we consider first, we assume that *all* of the matter that falls back has moved beyond the position of the secondary (in § 3.2 we shall critically assess this assumption). Therefore, the secondary can be polluted *twice* with supernova material, first by all the material that is ejected and then by material that falls back. We assume that the fraction of matter that is captured is given by the geometric fraction of the secondary $[(R_2^0/2a_0)^2 \simeq 0.01–0.03$, where $R_2^0 = 0.8\ R_\odot(M_2^0/M_\odot)^{0.8}$ is the radius of the secondary and a_0 is the initial orbital separation] times some efficiency factor f, where we assume different efficiency factors for matter that passes the secondary in the initial ejection ($f_{\rm ejection}$) and matter that falls back ($f_{\rm fallback}$). The efficiency factors can be much smaller than 1, for example, if the
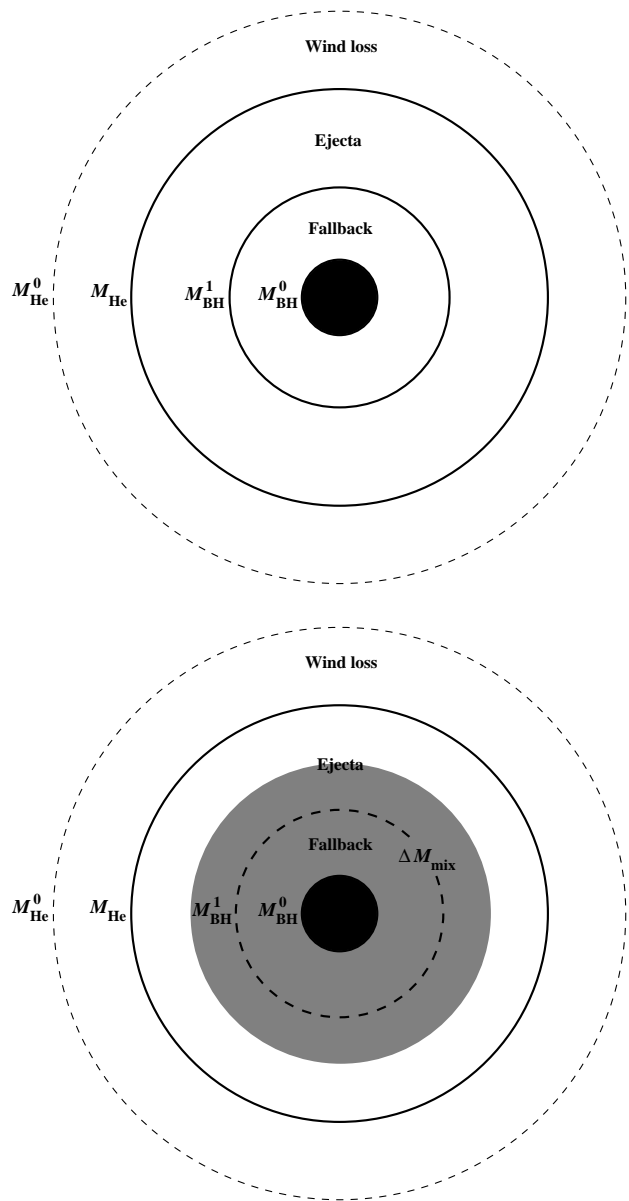

Fig. 3.—Schematic diagram defining the various mass parameters in (a) the simple fallback model and (b) the fallback with mixing model. $M_{\rm BH}^0$ is the initial black hole mass, $M_{\rm BH}^1$ the black hole mass after fallback, $M_{\rm He}$ the mass of the helium star at the time of the supernova, $M_{\rm He}^0$ the initial mass of the helium core (without wind mass loss), $\Delta M_{\rm mix}$ the mass in the mixing region (b).

supernova leads to stripping of matter from the secondary (Marietta, Burrows, & Fryxell 2000 and § 3.1), or larger than 1 if gravitational focusing is important. The latter requires that the relative velocity of the material is less than the escape velocity of the secondary and can plausibly occur only for fallback material. We also take into account the pollution of the secondary that has occurred before the supernova because of the capture of wind material by the secondary (where we assume a capture efficiency of 1).

The matter that is captured by the secondary has a much larger mean molecular weight than the composition of the secondary, a relatively unevolved star at this stage. This is secularly unstable and leads to thermohaline mixing in the secondary (e.g., Kippenhahn, Ruschenplatt, & Thomas 1980). Since the timescale for thermohaline mixing is short

---

[2] The term "hypernova" was coined by Paczyński (1998) as a model for gamma-ray bursters, linking them to the cataclysmic deaths of massive stars and the formation of black holes, as in the failed-supernova model of Woosley (1993) (for more details see MacFadyen & Woosley 1999). For the purposes of this study, we just define them as very energetic supernovae with energies $\gtrsim 10^{52}$ ergs, as has been used by Iwamoto et al. (1998) and Nomoto et al. (2001a, 2001b).

compared to the evolutionary timescale of the secondary, we assume that the material captured by the secondary is completely mixed with the rest of the star after the supernova.

In order to be able to follow the postsupernova evolution, we assume that the presupernova system is circular and that the supernova explosion is spherically symmetric in the frame of the primary. It is then straightforward to estimate the postsupernova parameters of the system (we follow Brandt & Podsiadlowski 1995, but for other equivalent treatments, see, e.g., Bhattacharya & van den Heuvel 1991; Nelemans et al. 1999). The eccentricity of the postsupernova binary is given by

$$ e = \frac{\Delta M_{\rm SN}}{M_{\rm BH}^1 + M_2^0} \, , $$

where $\Delta M_{\rm SN} \equiv M_{\rm He} - M_{\rm BH}^1$, and the postsupernova semimajor axis by

$$ a_{\rm PSN} = \frac{a_0}{1 - e} \, , $$

where a_0 is the initial orbital separation. The postsupernova system kick velocity can be obtained from equation (2.10) in Brandt & Podsiadlowski (1995) as

$$ v_{\rm sys} = v_{\rm orb}^0 \, \frac{\Delta M_{\rm SN}}{M_{\rm BH}^1 + M_2^0} \, \frac{M_2^0}{M_{\rm He} + M_2^0} \, , $$

where $v_{\rm orb}^0$ is the presupernova orbital velocity of the system. Here we have neglected the small change in the mass of the secondary due to the capture of ejected material from the primary (typically $\sim 0.2 \, M_\odot$), as well as any kick associated with the interaction of the supernova blast wave with the secondary (see Marietta et al. 2000).

After the supernova, the binary parameters will continue to evolve. The system will first recircularize, obtaining a new orbital separation

$$ a_{\rm rec} = a_{\rm PSN}(1 - e^2) \, . $$

Once the secondary starts to fill its Roche lobe, it will start to lose mass, of which a fraction β will be accreted by the primary, while the rest will be ejected from the system. We assume that the matter that is lost from the system carries away the same specific angular momentum as the primary (see, e.g., Podsiadlowski, Rappaport, & Pfahl 2002). This is appropriate if the mass loss occurs from a region near the primary, as suggested by the relativistic jets observed from Nova Sco (Hjellming & Rupen 1995).

Even though this model is still relatively simple (for example, it does not take into account a kick due to an asymmetric explosion), it still contains a large number of essentially unspecified parameters ($M_{\rm He}^0$, $M_{\rm BH}^0$, $M_{\rm fallback}$, $f_{\rm ejection}$, $f_{\rm fallback}$, g, and β). For given values of $f_{\rm ejection}$ and $f_{\rm fallback}$, we have sampled all the other parameters in a fairly systematic and comprehensive fashion, although we generally do not change the present masses of the Nova Sco components, but keep them fixed at 5.4 and 1.45 $M_\odot$, respectively.[3] In practice, we proceed in the following way. For each of the seven supernova models (i.e., each combination of helium star mass and explosion energy), we systematically vary the initial black hole mass, $M_{\rm BH}^0$; the

fallback mass, $M_{\rm fallback}$; the wind-loss parameter, g; and the mass-accretion parameters, β (the latter two are varied from 0 to 1). Having fixed these parameters, we can use the present orbital period and masses to reconstruct the presupernova masses and presupernova orbital period using the formalism outlined above. If this reconstruction shows that the radius of the presupernova secondary is smaller than its Roche lobe and that the system remains bound in the supernova explosion (if $e < 1$), we calculate the pollution and mixing in the secondary for our assumed values of $f_{\rm ejection}$ and $f_{\rm fallback}$. In order to decide whether an acceptable model has been found, we define a quality parameter as

$$ Q = \frac{1}{7} \sum_{i=1}^{7} \left(\frac{[{\rm X}_i/{\rm H}] - [{\rm X}_i/{\rm H}]^{\rm obs}}{\Delta[{\rm X}_i/{\rm H}]^{\rm obs}} \right)^2 \, , $$

where $[{\rm X}_i/{\rm H}]$ are the calculated logarithmic abundances (relative to solar) of N, O, Mg, Si, S, Ti, and Fe and $[{\rm X}_i/{\rm H}]^{\rm obs}$ are the abundances obtained by Israelian et al. (1999) and $\Delta[{\rm X}_i/{\rm H}]^{\rm obs}$ are the observational errors (see Table 1). We consider a particular model acceptable if $Q \leq 1$.

2.2. Results

In Table 2 we present the results for three combinations of $f_{\rm ejection}$ and $f_{\rm fallback}$ ([1, 1], [0, 1], and [0, 2]), for all supernova models that produced acceptable fits. The first two columns specify the initial mass of the helium star and the supernova explosion energy, while the next 10 columns give the mean logarithmic abundances (relative to solar) of He, C, O, Ne, Mg, Si, S, Ca, Ti, and Fe for acceptable models. The next six columns contain the mean values of selected model parameters (the mass of the He star just before the supernova, the initial mass of the compact star, the black hole mass after fallback, the initial mass of the secondary, the system kick velocity, and the maximum system kick velocity for each set of calculations, i.e., each of the seven supernova models). The last value, $N_{\rm tot}$, gives the total number of acceptable models for each supernova set and provides a measure of how easy it is to obtain an acceptable model for the pollution in the secondary for each set. All the quoted uncertainties are the standard deviations calculated for all acceptable models in each set. They are not proper statistical error estimates, since they are based on an even sampling of the unknown parameters. Nevertheless, they give an indication of the range of the corresponding model parameters.

Consistency with nucleosynthesis calculations.—As the table shows, many acceptable fits can be obtained for many plausible combinations of the parameters. In particular, acceptable fits can be found for He star models with $M_{\rm He}^0$ of 10 and 16 $M_\odot$ for all explosion energies. To some degree, this just reflects the fact that explosive nucleosynthesis produces similar overall abundance patterns in all of these models. Indeed, the overall consistency of the modeled abundances with the observed pollution in the secondary of Nova Sco provides confirmation of the general predictions of stellar and supernova nucleosynthesis.

The only exception to this picture is the abundance of Ti, which is too low by at least a factor of 2 in all models. This may be caused by errors in some of the nuclear cross sections used in the explosive nucleosynthesis calculation or could provide evidence for a more a complicated nucleosynthesis environment in the explosion (see § 3.5).

---

[3] We have also performed some calculations using masses of 6 and 2 $M_\odot$, respectively, obtaining similar results.

M_{He}^0 ($M_\odot$)	E_{SN} (foe)	He	C	O	Ne	Mg	Si	S	Ca	Ti	Fe	M_{He} ($M_\odot$)	M_{BH}^0 ($M_\odot$)	M_{BH}^1 ($M_\odot$)	M_2^0 ($M_\odot$)	v_{kick} (km s^{-1})	v_{kick}^{max} (km s^{-1})	N_{tot}
						Model A: Capture Models with Fallback ($f_{ejection} = 1$, $f_{fallback} = 1$, $M_2 = 1.45\ M_\odot$, $M_{BH} = 5.4\ M_\odot$)												
10.....	1	0.03 ±0.01	0.21 ±0.03	0.76 ±0.06	0.69 ±0.06	0.83 ±0.06	0.84 ±0.09	0.73 ±0.09	0.53 ±0.10	0.22 ±0.06	0.20 ±0.14	6.96 ±1.74	2.04 ±0.18	4.66 ±0.50	2.36 ±0.45	39 ±18	81	79242
16.....	1	0.02 ±0.00	0.11 ±0.03	0.92 ±0.10	0.65 ±0.09	0.89 ±0.10	0.85 ±0.10	0.74 ±0.11	0.59 ±0.14	0.19 ±0.08	0.19 ±0.14	8.21 ±2.03	2.74 ±0.23	4.93 ±0.34	2.04 ±0.35	46 ±19	90	64780
10.....	8	0.03 ±0.00	0.20 ±0.03	0.72 ±0.06	0.53 ±0.05	0.73 ±0.06	0.88 ±0.08	0.81 ±0.10	0.69 ±0.14	0.17 ±0.07	0.15 ±0.10	6.95 ±1.75	2.63 ±0.16	4.65 ±0.51	2.38 ±0.45	40 ±18	81	61514
10.....	30	0.03 ±0.00	0.21 ±0.02	0.65 ±0.03	0.36 ±0.02	0.62 ±0.02	0.91 ±0.06	0.85 ±0.09	0.74 ±0.13	0.15 ±0.05	0.10 ±0.05	7.10 ±1.74	3.61 ±0.14	4.68 ±0.49	2.45 ±0.40	44 ±20	81	16952
16.....	30	0.02 ±0.00	0.09 ±0.02	0.81 ±0.10	0.51 ±0.08	0.74 ±0.10	0.89 ±0.10	0.84 ±0.12	0.80 ±0.16	0.20 ±0.08	0.16 ±0.09	8.42 ±1.99	4.22 ±0.27	4.99 ±0.28	2.00 ±0.31	47 ±19	90	69290
						Model B: Capture Models with Fallback ($f_{capture} = 0$, $f_{fallback} = 1$, $M_2 = 1.45\ M_\odot$, $M_{BH} = 5.4\ M_\odot$)												
10.....	1	0.03 ±0.00	0.24 ±0.01	0.68 ±0.02	0.62 ±0.03	0.73 ±0.03	0.75 ±0.02	0.64 ±0.02	0.47 ±0.05	0.20 ±0.05	0.22 ±0.10	4.48 ±0.69	1.92 ±0.12	3.74 ±0.62	3.27 ±0.40	22 ±6	45	6996
16.....	1	0.02 ±0.00	0.12 ±0.02	0.87 ±0.08	0.63 ±0.08	0.85 ±0.09	0.77 ±0.05	0.65 ±0.06	0.54 ±0.07	0.19 ±0.08	0.24 ±0.14	6.95 ±1.49	2.58 ±0.21	4.66 ±0.37	2.38 ±0.29	42 ±17	90	28655
10.....	8	0.03 ±0.00	0.24 ±0.02	0.64 ±0.02	0.53 ±0.05	0.66 ±0.03	0.76 ±0.03	0.71 ±0.03	0.66 ±0.04	0.18 ±0.03	0.19 ±0.07	4.48 ±0.65	2.48 ±0.08	3.79 ±0.63	3.25 ±0.38	20 ±5	36	4200
10.....	30	0.03 ±0.00	0.23 ±0.01	0.59 ±0.03	0.38 ±0.01	0.61 ±0.02	0.81 ±0.05	0.77 ±0.08	0.72 ±0.10	0.29 ±0.14	0.24 ±0.10	4.40 ±0.72	3.01 ±0.35	3.81 ±0.76	3.34 ±0.48	18 ±7	26	1317
16.....	30	0.02 ±0.00	0.10 ±0.02	0.77 ±0.09	0.55 ±0.06	0.76 ±0.08	0.76 ±0.06	0.71 ±0.08	0.74 ±0.10	0.24 ±0.10	0.26 ±0.13	7.00 ±1.29	3.85 ±0.31	4.82 ±0.27	2.29 ±0.23	38 ±17	84	32257
						Model C: Capture Models with Fallback ($f_{capture} = 0$, $f_{fallback} = 2$, $M_2 = 1.45\ M_\odot$, $M_{BH} = 5.4\ M_\odot$)												
10.....	1	0.02 ±0.01	0.16 ±0.07	0.69 ±0.06	0.61 ±0.06	0.76 ±0.06	0.85 ±0.08	0.75 ±0.08	0.54 ±0.10	0.21 ±0.05	0.17 ±0.12	6.58 ±1.74	2.07 ±0.16	4.57 ±0.54	2.48 ±0.45	37 ±19	81	54039
16.....	1	0.02 ±0.00	0.10 ±0.02	0.84 ±0.11	0.57 ±0.10	0.81 ±0.11	0.85 ±0.09	0.76 ±0.11	0.61 ±0.14	0.19 ±0.08	0.18 ±0.14	7.73 ±1.87	2.77 ±0.21	4.85 ±0.34	2.14 ±0.32	44 ±19	90	49459
10.....	8	0.03 ±0.01	0.19 ±0.06	0.67 ±0.05	0.45 ±0.08	0.66 ±0.05	0.90 ±0.07	0.84 ±0.08	0.73 ±0.12	0.17 ±0.07	0.15 ±0.08	5.78 ±1.48	2.63 ±0.13	4.44 ±0.62	2.69 ±0.45	27 ±15	81	22673
10.....	30	0.03 ±0.00	0.22 ±0.01	0.61 ±0.03	0.38 ±0.02	0.62 ±0.02	0.83 ±0.07	0.78 ±0.08	0.72 ±0.10	0.22 ±0.08	0.18 ±0.10	4.51 ±0.67	3.37 ±0.27	3.92 ±0.69	3.18 ±0.35	17 ±5	26	1617
16.....	30	0.02 ±0.00	0.10 ±0.02	0.75 ±0.10	0.53 ±0.07	0.73 ±0.10	0.85 ±0.09	0.82 ±0.12	0.83 ±0.13	0.21 ±0.08	0.19 ±0.09	6.99 ±1.24	4.16 ±0.22	4.82 ±0.29	2.23 ±0.25	37 ±16	81	30943

NOTE.—M_{He}^0: initial helium star mass; E_{SN}: explosion energy (1 foe $\equiv 10^{51}$ ergs); He, C,..., Fe: logarithmic abundances (relative to solar) of He, C,..., Fe; M_{He}: presupernova helium star mass; M_{BH}^0: initial mass of the compact remnant; M_{BH}^1: black hole mass after fallback; M_2^0: initial mass of the secondary; v_{kick}: system kick velocity; v_{kick}^{max}: maximum system kick velocity for each supernova set; N_{tot}: total number of acceptable models for each supernova set.

In Table 4 we summarize some of the key binary parameters of the best-fit models for models A, B, and C in Table 2. Note particularly that the initial separation before the supernova is typically less than 6 $R_\odot$, much smaller than the present separation (15.2 $R_\odot$). This implies that the secondary was almost filling its Roche lobe before the supernova and results in a relatively large geometrical cross section for the capture of material from the supernova ejecta ($\sim$0.26 $M_\odot$). The semimajor axis of the post-supernova system is only slightly increased (at least in models where the black hole receives no kick at birth). Hence there had to be substantial mass transfer ($\sim$1 $M_\odot$) after the supernova to widen the system to the present separation.

The model also predicts some other abundance anomalies. The abundance of C is predicted to be enhanced by up to a factor of 1.7, the abundance of Ca by a factor of 3–7, and the abundance of Ne by a factor of 2–5. The enhancement of Ca is weakly correlated and the enhancement of Ne is weakly anticorrelated with the explosion energy (these correlations are strongest for the 10 $M_\odot$ models). Therefore, these patterns provide, at least in principle, a means by which one could distinguish between a normal supernova and a hypernova event.

Requirement of fallback.—All models require some fallback, where hypernova models require the smallest amount. This is the result of two factors: (1) The initial black hole mass must be close to the mass cut since matter near the mass cut (which is much smaller than the present black hole mass) must have been ejected in order to produce the observed abundances. The mass cut is a function of the mass of the helium star and the energy of the explosion and is largest for the 16 $M_\odot$ hypernova model (see Fig. 1). (2) The black hole mass cannot increase by much more than $\sim$1 $M_\odot$ by mass accretion from the secondary after the supernova. This is a consequence of the constraints on the presupernova orbital parameters imposed by the present orbital separation and component masses. A larger amount of postsupernova mass transfer implies a tighter presupernova binary (because mass transfer widens the system). The largest amount of mass transfer is therefore determined by the condition that the presupernova secondary just fills its Roche lobe. We note that this constraint would be substantially weaker if we had allowed for an asymmetric supernova explosion.

Low system kick velocities.—The typical system kick velocities are relatively low, varying from 10 to 60 km s^{-1}. There are a few extreme cases for the 16 $M_\odot$ models where the system velocity is as high as $\sim$90 km s^{-1}. However, these cases are very rare and require very special model parameters. These are cases where the helium star loses relatively little of its envelope in a stellar wind before the supernova ($M_{\rm He} \gtrsim 13$ $M_\odot$) and where the system becomes almost unbound in the supernova event (the immediate postsupernova eccentricity is close to 1). Whether such a small amount of wind mass loss is physically reasonable is somewhat doubtful. In any case, since the parameter range that leads to these high kick velocities is extremely limited, such solutions, while not formally ruled out, are statistically not favored. The minimum observed space velocity of Nova Sco is 106 km s^{-1} and possibly much larger, since this corresponds to the radial velocity only. It therefore appears very unlikely that a symmetric supernova explosion alone could explain the observed velocity. This implies that an additional kick, e.g., due to an asymmetry in the explosion, is required. While our model did not take this possibility into account, our results are consistent with it. The initial masses of the compact remnant, $M_{\rm BH}^0$, for many of the helium star models with a mass of 10 $M_\odot$ and for normal supernova explosions are consistent with the maximum mass allowed for neutron stars. Even when $M_{\rm BH}^0$ is larger than the maximum mass of a neutron star, a neutron star may have formed first, since, in our simple model, $M_{\rm BH}^0$, strictly speaking, does not only include the initial mass of the compact remnant, but also any fallback material that did not reach the orbit of the secondary. Therefore, a two-stage process where the collapse first leads to the formation of a neutron star, accompanied by a supernova kick, which is subsequently converted into a black hole by fallback may well explain the observed space velocity (see Brandt et al. 1995).

We note that these conclusions are not inconsistent with the findings of Nelemans et al. (1999). Their results also imply that one requires rather *special* parameters to explain the observed space velocity of Nova Sco with a *symmetric* supernova explosion alone. In addition, some of the sets of parameters they present for illustration can be ruled out by the present investigation, which takes into account more observational constraints and the reduced masses of the Nova Sco components.

3. DISCUSSION

In the previous section we showed that a relatively simple model can explain most of the observed α-element enhancements in the secondary of Nova Sco. We now turn to an examination of the question whether some of the assumptions that went into the model are actually physically reasonable.

3.1. *Capture Efficiency*

Obviously, a significant fraction of the supernova ejecta must have been captured by the secondary. This is not necessarily expected. Marietta et al. (2000) recently examined the effects of a supernova blast wave on a binary companion in the context of a Type Ia supernova. They showed that a significant part of the outer part of the secondary was lost by ram-pressure stripping. Instead of accreting matter from the supernova ejecta, the secondary actually lost mass. On the other hand, the layers in which α-process elements are synthesized are buried deep inside the core and move with a much lower velocity than the outer layers of the helium star, which are mainly responsible for the ram-pressure stripping. This makes it easier for some of that material to be captured by the secondary (see the discussion in Marietta et al. 2000).

The problem is less severe if the material captured comes mainly from fallback since this material will generally have a much lower velocity than the escaping material. Indeed, if the velocity relative to the secondary is smaller than the escape velocity at the surface of the secondary, gravitational focusing could increase the capture efficiency above a value of 1.

3.2. *The Requirement of Fallback*

Substantial fallback is commonly found in supernova explosions with hydrogen-rich envelopes (see Woosley & Weaver 1995). This fallback occurs either because matter (typically just above the mass cut) did not attain escape

speed in the supernova or, more significantly, because it was pushed back by hydrodynamical effects, in particular, by a reverse shock that forms at the interface of the He/H boundary. However, in the present model there is no hydrogen envelope to produce the interface for a strong reverse shock. A strong reverse shock is also formed at the CO/He interface as seen in Type Ib supernova models (Hachisu et al. 1991, 1994). In the absence of a strong reverse shock from the composition interface, the natural location for fallback, if it occurs, is close to the original core and not close to the location of the secondary (as required in our simple model) (unless the system is still surrounded by a common envelope, which cannot be completely ruled out, but is a priori very unlikely).

3.3. *Fallback with Mixing?*

A possible solution to this problem is a modification of our model where fallback occurs from a region near the core, but is accompanied by substantial mixing. Some of this mixed material, enriched with α-element–rich material near the mass cut, is ejected and produces the observed pollution in the secondary, while the rest falls back onto the compact remnant (see Fig. 2, case B).

There are several scenarios in which such mixing could arise.

1. In some of the collapsar model studied by MacFadyen, Woosley, & Heger (2001), the initial collapse leads to the formation of a neutron star and a weak supernova shock that fails to eject all of the helium core. As the shock stalls, matter falls back onto the core converting the neutron star into a black hole. The energy that is associated with this collapse may then be able to eject the outer envelope (perhaps in the form of jet-powered shocks; for a similar suggestion for Nova Sco, see Brown et al. 2000). Vigorous mixing is expected to occur in this scenario, since, as material tries to fall back, it is being pushed up by a low-density neutrino-heated bubble, which is Rayleigh-Taylor unstable (see, e.g., Kifonidis et al. 2000).

2. If a black hole forms promptly, mixing in the ejecta may be induced by Rayleigh-Taylor instabilities at the Si/O interface (Kifonidis et al. 2000; Kifonidis 2001) as well as the CO/He interface (Hachisu et al. 1991, 1994). After mixing, the inner part of the mixed layers may fall back, increasing the mass of the initial black hole. Umeda & Nomoto (2002) have shown that such mixing followed by fallback can explain the large Zn abundance observed in very metal poor stars and suggested that this may be a generic feature of core-collapse supernovae, involving the formation of either a black hole or a neutron star.

3. In an aspherical explosion, heavy elements synthesized in a deep layer may be mixed into outer layers in the form of a jet (Maeda et al. 2002), while fallback occurs from the equatorial region. This is equivalent to the mixing and fallback process discussed in Umeda & Nomoto (2002) and could occur for the formation of both a black hole or a neutron star.

Such a scenario has several advantages: (1) A neutron star may form first, and the associated neutrino emission can be responsible for a standard neutrino-induced supernova kick to explain the observed space velocity. (2) Material near the mass cut is mixed into the envelope and can escape with it, explaining the abundance

anomalies in the secondary. (3) The supernova explosion could be weaker and ram-pressure stripping would then be less of a problem; this could allow for more efficient capture of supernova material by the secondary (even in the case of a hypernova explosion, the ejecta in the equatorial plane could be moving relatively slowly).

3.4. *Case B: Fallback with Mixing Simulations*

In order to simulate a fallback model with mixing, we modified the model described in § 2.1 by assuming that the layer between M_{BH}^0 and $M_{BH}^0 + \Delta M_{mix}$ is completely mixed during the collapse phase, where we defined $\Delta M_{mix} \equiv m M_{fallback}$ (see Fig. 3b). The definition of M_{BH}^0 includes both the initial mass of the compact remnant and any fallback material that was not mixed with the material that is ejected (this could, for example, be material from the inner parts of the disk that forms around the initial compact core, as in the collapsar models of MacFadyen & Woosley [1999] and MacFadyen et al. [2001] or material falling back from the equatorial region of the star in an aspherical explosion [Maeda et al. 2002]).

In Table 3 we present the results of these simulations for $m = 1, 2, 3$, and 4. Most of the results are similar to the earlier calculations: the amount of fallback is similar, while the system velocities tend to be a bit larger. One significant difference is that, with the inclusion of mixing, hypernova models are preferred over standard supernova models, which tend not to produce enough S.

The size of the mixing region outside the initial compact remnant varies quite significantly between different models; in some hypernova models, the mixing region contains less than 1 $M_\odot$, while in normal supernova models at least several $M_\odot$ are required.

3.5. *Case C: Nonspherical Models*

So far, we have assumed that the ejection of matter occurs in a more or less spherically symmetric way. However, this is not generally expected for hypernova or collapsar models, in particular, those associated with gamma-ray bursts (MacFadyen & Woosley 1999). In these models it is generally believed that the core is initially rapidly rotating and that the accretion of matter onto the compact object occurs through an accretion disk. Maeda et al. (2002) have recently constructed aspherical hypernova models for the hypernova SN 1998bw, simulating both the hydrodynamics and the nucleosynthesis in two dimensions for a helium star model of 16 $M_\odot$ at the beginning of helium burning. They showed that the chemical composition of the ejecta is strongly dependent on direction. In particular, Fe is mainly ejected in the polar direction, while O and Mg are preferentially ejected near the equatorial plane.

To simulate the pollution by an aspherical hypernova, we assume that the secondary is located in the equatorial plane of the helium star (and the black hole accretion disk) and that the secondary captures material that is within an angle θ of the equatorial plane, where θ is the angular radius subtended by the secondary as seen from the helium star. The results of these simulations (for their best model C) are presented in Tables 4 and 5 and are indicated by an asterisk (*). Somewhat surprisingly, none of our simulations produced acceptable fits (the results shown were obtained by increasing the acceptance parameter Q from 1 to 2). This is a direct consequence of the large overabundance of O and Mg near the equatorial plane. All models produce either an

TABLE 3

ACCEPTABLE MIXING MODELS FOR THE SECONDARY OF NOVA SCO

$M_{\rm He}^0$ ($M_\odot$)	$E_{\rm SN}$ (foe)	He	C	O	Ne	Mg	Si	S	Ca	Ti	Fe	$M_{\rm He}$ ($M_\odot$)	$M_{\rm BH}^0$ ($M_\odot$)	$M_{\rm BH}^1$ ($M_\odot$)	M_2^0 ($M_\odot$)	$\Delta M_{\rm mix}$ ($M_\odot$)	$v_{\rm kick}$ (km s^{-1})	$v_{\rm kick}^{\rm max}$ (km s^{-1})	$N_{\rm tot}$
Model D: Capture Models with Mixing ($f_{\rm capture} = 1$, $\Delta M_{\rm mix} = M_{\rm fallback}$, $M_2 = 1.45\ M_\odot$, $M_{\rm BH} = 5.4\ M_\odot$)																			
10......	30	0.03 ±0.00	0.23 ±0.00	0.63 ±0.01	0.39 ±0.00	0.64 ±0.01	0.87 ±0.04	0.83 ±0.06	0.77 ±0.08	0.20 ±0.06	0.17 ±0.07	3.94 ±0.15	2.57 ±0.42	3.27 ±0.15	3.58 ±0.15	0.71 ±0.42	22 ±2	25	7396
16......	30	0.02 ±0.00	0.12 ±0.01	0.93 ±0.05	0.62 ±0.04	0.87 ±0.04	0.83 ±0.09	0.71 ±0.13	0.61 ±0.17	0.13 ±0.07	0.10 ±0.07	6.05 ±0.91	3.40 ±0.57	4.34 ±0.24	2.59 ±0.22	0.94 ±0.57	37 ±13	66	27814
Model E: Capture Models with Mixing ($f_{\rm capture} = 1$, $\Delta M_{\rm mix} = 2\ M_{\rm fallback}$, $M_2 = 1.45\ M_\odot$, $M_{\rm BH} = 5.4\ M_\odot$)																			
16......	1	0.03 ±0.00	0.15 ±0.01	0.97 ±0.03	0.74 ±0.03	0.96 ±0.03	0.70 ±0.02	0.50 ±0.01	0.42 ±0.02	0.15 ±0.03	0.19 ±0.07	7.01 ±1.20	2.54 ±0.14	4.43 ±0.35	2.50 ±0.28	3.78 ±0.84	53 ±11	76	1828
10......	30	0.03 ±0.00	0.23 ±0.00	0.63 ±0.01	0.39 ±0.00	0.63 ±0.01	0.83 ±0.05	0.79 ±0.06	0.73 ±0.07	0.26 ±0.10	0.27 ±0.11	3.98 ±0.28	2.91 ±0.29	3.28 ±0.21	3.57 ±0.21	0.74 ±0.40	23 ±3	35	4035
16......	30	0.02 ±0.00	0.11 ±0.01	0.86 ±0.07	0.58 ±0.05	0.82 ±0.06	0.75 ±0.07	0.63 ±0.07	0.61 ±0.08	0.31 ±0.18	0.28 ±0.14	8.24 ±1.97	3.44 ±0.54	4.80 ±0.35	2.17 ±0.32	2.73 ±1.35	54 ±18	90	80486
Model F: Capture Models with Mixing ($f_{\rm capture} = 1$, $\Delta M_{\rm mix} = 3\ M_{\rm fallback}$, $M_2 = 1.45\ M_\odot$, $M_{\rm BH} = 5.4\ M_\odot$)																			
16......	1	0.02 ±0.00	0.12 ±0.01	0.88 ±0.02	0.65 ±0.02	0.87 ±0.02	0.69 ±0.02	0.54 ±0.02	0.45 ±0.03	0.16 ±0.04	0.20 ±0.09	10.71 ±0.84	2.55 ±0.16	5.01 ±0.14	1.90 ±0.09	7.38 ±0.69	80 ±5	90	2353
10......	8	0.03 ±0.00	0.24 ±0.00	0.69 ±0.00	0.57 ±0.00	0.72 ±0.00	0.70 ±0.00	0.61 ±0.01	0.52 ±0.02	0.12 ±0.01	0.10 ±0.01	3.59 ±0.02	2.55 ±0.02	2.88 ±0.02	3.97 ±0.02	0.98 ±0.06	26 ±0	36	36
10......	30	0.03 ±0.00	0.23 ±0.00	0.63 ±0.01	0.39 ±0.01	0.63 ±0.01	0.84 ±0.05	0.80 ±0.06	0.73 ±0.08	0.20 ±0.05	0.19 ±0.08	4.13 ±0.37	3.19 ±0.14	3.40 ±0.20	3.45 ±0.20	0.61 ±0.46	23 ±5	45	1694
16......	30	0.02 ±0.00	0.11 ±0.02	0.84 ±0.07	0.56 ±0.06	0.80 ±0.07	0.77 ±0.07	0.68 ±0.07	0.66 ±0.09	0.27 ±0.17	0.26 ±0.15	8.97 ±1.97	3.68 ±0.50	4.89 ±0.33	2.06 ±0.31	3.63 ±1.98	60 ±17	90	62403
Model G: Capture Models with Mixing ($f_{\rm capture} = 1$, $\Delta M_{\rm mix} = 4\ M_{\rm fallback}$, $M_2 = 1.45\ M_\odot$, $M_{\rm BH} = 5.4\ M_\odot$)																			
16......	1	0.02 ±0.00	0.13 ±0.00	0.90 ±0.00	0.67 ±0.00	0.89 ±0.00	0.70 ±0.01	0.53 ±0.01	0.38 ±0.01	0.08 ±0.00	0.06 ±0.02	11.60 ±0.00	2.84 ±0.02	5.01 ±0.00	1.84 ±0.00	8.67 ±0.06	90 ±0	90	11
10......	30	0.03 ±0.00	0.23 ±0.00	0.63 ±0.01	0.39 ±0.01	0.63 ±0.01	0.85 ±0.04	0.81 ±0.06	0.75 ±0.08	0.20 ±0.05	0.18 ±0.08	4.04 ±0.24	3.23 ±0.14	3.35 ±0.16	3.50 ±0.16	0.48 ±0.32	23 ±3	35	1052
16......	30	0.02 ±0.00	0.11 ±0.02	0.85 ±0.07	0.56 ±0.06	0.80 ±0.07	0.79 ±0.07	0.70 ±0.08	0.66 ±0.11	0.19 ±0.10	0.19 ±0.13	9.11 ±2.04	3.95 ±0.36	4.89 ±0.33	2.05 ±0.32	3.74 ±2.13	61 ±17	90	39602

NOTE.—$\Delta M_{\rm mix}$: mass of the mixing region above $M_{\rm BH}^0$; all other columns are as in Table 2.

TABLE 4

BINARY PARAMETERS FOR "BEST-FIT" MODELS

Model	M_{He}^0 $(M_\odot)$	E_{SN}	M_{He} $(M_\odot)$	M_{BH}^0 $(M_\odot)$	M_{BH}^1 $(M_\odot)$	M_2^0 $(M_\odot)$	a_{pre} $(R_\odot)$	a_{post} $(R_\odot)$	e	f_{geo}	$M_{capture}$ $(M_\odot)$	v_{kick} (km s^{-1})
Fallback Models												
A	10	1	5.57	2.22	5.07	2.76	5.68	6.06	0.06	0.025	0.27	11
B	16	30	5.56	3.94	4.40	2.78	5.84	6.96	0.16	0.024	0.26	28
C	16	30	5.54	4.06	4.38	2.81	5.79	6.91	0.16	0.025	0.28	28
A*	16	10	4.96	2.40	3.75	3.10	5.84	7.10	0.18	0.029	0.51	35
B*	16	10	5.50	2.40	4.35	2.85	5.73	6.82	0.16	0.026	0.37	29
A′	16	10	6.20	4.30	5.11	2.61	5.66	6.59	0.14	0.023	0.29	23
B′	16	10	6.61	2.48	4.26	2.59	5.68	8.65	0.34	0.023	0.25	54
Mixing Models												
D	16	30	3.81	3.80	3.81	3.04	6.93	6.93	0.00	0.020	0.24	0
E	16	30	6.63	3.81	4.28	2.57	5.73	8.70	0.34	0.022	0.26	53
F	16	30	6.89	3.89	4.61	2.50	5.66	8.33	0.32	0.022	0.25	48
G	16	30	8.00	3.94	4.57	2.28	5.71	11.43	0.50	0.018	0.21	65
E*	16	10	6.58	2.40	4.26	2.60	5.69	8.61	0.34	0.023	0.30	53
F*	16	10	10.45	2.40	5.01	1.96	5.56	25.08	0.78	0.015	0.20	80
E′	16	10	6.61	2.46	4.26	2.59	5.68	8.65	0.34	0.023	0.26	54
F′	16	10	9.24	2.48	4.74	2.12	5.59	16.33	0.66	0.017	0.19	76

NOTE.—The present masses of the black hole and the secondary in the Nova Sco system are assumed to be 5.4 and 1.45 $M_\odot$, respectively, implying a present orbital separation of 15.2 $R_\odot$. a_{pre}/a_{post}: pre-/postsupernova semimajor axis; e: postsupernova eccentricity; f_{geo}: presupernova fractional, geometrical cross section of the secondary; $M_{capture}$: total mass captured by the secondary; all other parameters are the same as in Tables 2 and 3.

unacceptable overabundance of O and Mg or an unacceptable underabundance of S and Si, depending on where the cutoff below which matter can be mixed into the ejecta occurs.

However, when modeling the shapes of spectral lines in SN 1998bw, Maeda et al. (2002) found that the fits could be improved if there was some lateral mixing in the ejecta, i.e., between material ejected in the equatorial plane and material ejected more along the jet axis (e.g., due to a shear instability). To test this possibility, we also considered a model where we assumed complete lateral mixing in the ejecta for the same hypernova model as used above, i.e., where all the material within given velocity bins was assumed to be mixed completely. The results of these simulations are also shown in Tables 4 and 5 and indicated with a prime ('). In this case, excellent fits are obtained, as one would have expected, since this model should approximate the spherical hypernova model used earlier. Interestingly, the Ti abundance is significantly enhanced ([Ti/H] ~ 0.5) and is marginally consistent with the observed value ([Ti/H] $\sim 0.9 \pm 0.4$). This increased Ti abundance comes at the price of an increased Fe abundance. While both the Ti and Fe abundances are consistent with the observed values, the ratio [Ti/Fe] is still significantly below the observed one (~ 0.2 instead of 0.8). We emphasize that the assumption of complete lateral mixing is extreme; at present we cannot identify any physical process that would lead to such a result. We note, however, that Höflich, Khokhlov, & Wang (2001) have shown that the jet in an aspherical supernova model is decelerated at the H/He interface and that material spreads laterally, although only to a limited extent. Whether this could provide a viable model requires computations with much higher numerical resolution. Irrespective of this, our results suggest that the enhanced abundance of Ti (which results from a mixture of the nucleosynthesis pro-

ducts of complete and incomplete Si burning; see Umeda & Nomoto 2002 for a discussion) could potentially provide a signature for an asymmetric hypernova.

4. CONCLUSIONS

The main conclusion of this investigation is that using standard supernova models and a relatively simple model for the pollution of the secondary, we can explain the observed α-element enhancements in the secondary of Nova Sco, confirming standard nucleosynthesis predictions (apart from the abundance of Ti, which is always too low).

Nova Sco presents a clear case for a two-step black hole formation process, where a substantial fraction of the black hole mass is the result of fallback. In order for the secondary to be polluted with material near the mass cut, this fallback material must either have reached the location of the secondary before falling back or, more likely, be mixed during the explosion with material that will escape. A two-step black hole formation process may provide a simple explanation for the high space velocity of Nova Sco, since the system may have received the same type of neutrino-induced kick as normal neutron stars are believed to. Alternatively, asymmetric mass ejection in an aspherical supernova/hypernova model may also contribute to the observed space velocity.

Our analysis shows that helium star models of 10–16 $M_\odot$ are most probable and that both normal supernova as well as more energetic hypernova models can explain the abundances observed in the secondary. The majority of acceptable models are, however, hypernova models, in particular for the more realistic models that include mixing. The one aspherical hypernova model we used only provided an acceptable fit to the observed abundance anomalies when we assumed that there was extreme lateral mixing between the ejecta in the equatorial plane and in the polar direction.

TABLE 5

BEST FALLBACK/MIXING MODELS FOR ASPHERICAL HYPERNOVA MODELS

M_{He}^0 ($M_\odot$)	E_{SN}	He	C	O	Ne	Mg	Si	S	Ca	Ti	Fe	M_{He} ($M_\odot$)	M_{BH}^0 ($M_\odot$)	M_{BH}^1 ($M_\odot$)	M_2^0 ($M_\odot$)	ΔM_{mix} ($M_\odot$)	v_{kick} (km s^{-1})	v_{kick}^{max} (km s^{-1})	N_{tot}
								No Lateral Mixing											
Model A*: Capture Models with Fallback ($f_{ejection} = 1$, $f_{fallback} = 1$, $M_2 = 1.45\ M_\odot$, $M_{BH} = 5.4\ M_\odot$)																			
16.....	10	0.02 ±0.00	0.16 ±0.03	1.12 ±0.08	0.79 ±0.07	0.97 ±0.07	0.66 ±0.06	0.43 ±0.06	0.32 ±0.06	0.08 ±0.02	0.08 ±0.02	8.00 ±2.05	2.51 ±0.07	4.83 ±0.37	2.17 ±0.35		49 ±19	90	...
Model B*: Capture Models with Fallback ($f_{capture} = 0$, $f_{fallback} = 1$, $M_2 = 1.45\ M_\odot$, $M_{BH} = 5.4\ M_\odot$)																			
16.....	10	0.03 ±0.00	0.17 ±0.01	1.06 ±0.03	0.76 ±0.04	0.91 ±0.03	0.58 ±0.02	0.36 ±0.01	0.27 ±0.01	0.08 ±0.01	0.07 ±0.01	5.88 ±0.85	2.44 ±0.03	4.36 ±0.44	2.72 ±0.23		35 ±10	66	...
Model E*: Capture Models with Mixing ($f_{capture} = 1$, $\Delta M_{mix} = 2\ M_{fallback}$, $M_2 = 1.45\ M_\odot$, $M_{BH} = 5.4\ M_\odot$)																			
16.....	10	0.03 ±0.00	0.17 ±0.00	1.04 ±0.01	0.76 ±0.01	0.89 ±0.01	0.48 ±0.00	0.24 ±0.00	0.18 ±0.00	0.06 ±0.00	0.06 ±0.00	6.70 ±0.13	2.43 ±0.02	4.40 ±0.16	2.54 ±0.04	3.94 ±0.32	50 ±2	53	...
Model F*: Capture Models with Mixing ($f_{capture} = 1$, $\Delta M_{mix} = 3\ M_{fallback}$, $M_2 = 1.45\ M_\odot$, $M_{BH} = 5.4\ M_\odot$)																			
16.....	10	0.03 ±0.00	0.14 ±0.01	0.96 ±0.02	0.67 ±0.02	0.81 ±0.02	0.47 ±0.01	0.26 ±0.01	0.19 ±0.01	0.06 ±0.00	0.05 ±0.00	10.89 ±0.65	2.45 ±0.03	5.03 ±0.13	1.89 ±0.07	7.75 ±0.41	82 ±4	90	...
								Complete Lateral Mixing											
Model A': Capture Models with Fallback ($f_{ejection} = 1$, $f_{fallback} = 1$, $M_2 = 1.45\ M_\odot$, $M_{BH} = 5.4\ M_\odot$)																			
16.....	10	0.02 ±0.00	0.11 ±0.02	0.90 ±0.09	0.58 ±0.07	0.74 ±0.08	0.71 ±0.11	0.63 ±0.11	0.63 ±0.10	0.55 ±0.07	0.37 ±0.07	8.25 ±2.03	3.38 ±0.64	4.91 ±0.34	2.09 ±0.34		49 ±19	90	637665
Model B': Capture Models with Fallback ($f_{capture} = 0$, $f_{fallback} = 1$, $M_2 = 1.45\ M_\odot$, $M_{BH} = 5.4\ M_\odot$)																			
16.....	10	0.03 ±0.00	0.11 ±0.02	0.86 ±0.07	0.56 ±0.07	0.71 ±0.07	0.63 ±0.06	0.55 ±0.07	0.54 ±0.06	0.51 ±0.05	0.30 ±0.04	6.64 ±1.34	3.03 ±0.48	4.62 ±0.38	2.44 ±0.28		38 ±16	90	177557
Model E': Capture Models with Mixing ($f_{capture} = 1$, $\Delta M_{mix} = 2\ M_{fallback}$, $M_2 = 1.45\ M_\odot$, $M_{BH} = 5.4\ M_\odot$)																			
16.....	10	0.03 ±0.00	0.12 ±0.01	0.89 ±0.05	0.60 ±0.04	0.74 ±0.04	0.59 ±0.04	0.49 ±0.05	0.50 ±0.04	0.51 ±0.03	0.28 ±0.03	7.78 ±1.88	3.43 ±0.64	4.69 ±0.37	2.31 ±0.32	2.53 ±1.52	53 ±18	90	195131
Model F': Capture Models with Mixing ($f_{capture} = 1$, $\Delta M_{mix} = 3\ M_{fallback}$, $M_2 = 1.45\ M_\odot$, $M_{BH} = 5.4\ M_\odot$)																			
16.....	10	0.03 ±0.00	0.12 ±0.01	0.88 ±0.05	0.59 ±0.05	0.73 ±0.05	0.59 ±0.04	0.49 ±0.05	0.50 ±0.04	0.51 ±0.03	0.28 ±0.03	8.56 ±2.04	3.65 ±0.61	4.78 ±0.35	2.19 ±0.33	3.41 ±2.33	60 ±18	90	141353

NOTE.—See Tables 2 and 3 for definitions.

Of course, so far we only tried one helium star model with a mass of 16 $M_\odot$ for one particular explosion energy. It is quite possible that for a lower mass model, the oxygen produced in the equatorial plane would be lower, while still preserving most of the hypernova features without requiring extreme lateral mixing. The modeling of the pollution for the aspherical explosion is clearly even more uncertain than in the spherical case, which suggests that it is important to study mixing processes in aspherical models with much higher numerical resolution.

On the other hand, it is also worth noting that it is not necessarily expected that the helium star progenitor of the black hole was rapidly rotating, since the progenitor is likely to have passed through an extended red supergiant phase before the system experienced a common-envelope and spiral-in phase. It is quite likely that in the red supergiant phase, the helium core would have been significantly spun down by both hydrodynamic (Heger, Langer, & Woosley 2000) and magnetohydrodynamic processes (Spruit & Phinney 1998), which efficiently couple the core to the slowly rotating, convective envelope (as may also be required to explain the low initial spin periods of the majority of radio pulsars in supernova remnants). Strohmayer (2001) has provided some evidence that the black hole may be rotating rapidly at the present time (based on observations of quasi-periodic oscillations at 450 Hz). However, as our modeling has shown, the black hole is likely to have accreted $\sim 1\ M_\odot$ after the supernova from the companion star (also see Beer & Podsiadlowski 2002). Since this accretion would also have spun up the black hole, the observations by Strohmayer (2001) do not provide a strong constraint on the rotation of the black hole at birth.

It is interesting to speculate on the relation between Nova Sco and other low-mass black hole binaries. Most low-mass black hole binaries have rather low space velocities, entirely consistent with the expected velocity dispersion caused by scattering by molecular clouds and spiral arms (Brandt et al. 1995). This may suggest that the black holes in these systems formed promptly, i.e., without a kick or significant mass ejection (see, however, the discussion in Nelemans et al. 1999 for a rather different point of view). This would then imply that the secondaries in these systems should not show the same enhancement in α-process elements as the secondary in Nova Sco, a prediction that should be checked with future high-resolution spectral observations of these systems. Orosz et al. (2001) recently reported the discovery of similar overabundances of α-process elements in the B star secondary of another X-ray transient, J1819.3$-$2525 (V4641 Sgr). Interestingly, this system also appears to have an anomalously high space velocity (its measured γ-velocity is 107 km s^{-1}). Unfortunately, this velocity estimate is quite uncertain at present because of the proximity of the system to the Galactic center, which makes the distance estimate very sensitive to the precise distance. Nevertheless, if confirmed, it would suggest that the system may have experienced a similar evolutionary history as Nova Sco.

REFERENCES

Bailyn, C. D., et al. 1995, Nature, 374, 701
Beer, M., & Podsiadlowski, Ph. 2002, MNRAS, in press (astro-ph/0109136)
Bhattacharya, D., & van den Heuvel, E. P. J. 1991, Phys. Rep., 203, 1
Brandt, W. N., & Podsiadlowski, Ph. 1995, MNRAS, 274, 461
Brandt, W. N., Podsiadlowski, Ph., & Sigurdsson, S. 1995, MNRAS, 277, L35
Brown, G. E., & Bethe, H. A. 1994, ApJ, 423, 659
Brown, G. E., Lee, C.-H., Wijers, R. A. M. J., Lee, H. K., Israelian, G., & Bethe, H. A. 2000, NewA, 5, 191
Fryer, C. L., & Kalogera, V. 2001, ApJ, 554, 548
Gourgoulhon, E., & Haensel, P. 1993, A&A, 271, 187
Hachisu, I., Matsuda, T., Nomoto, K., & Shigeyama, T. 1991, ApJ, 368, L27
———. 1994, A&AS, 104, 341
Harmon, B. A., et al. 1995, Nature, 374, 703
Heger, A., Langer, N., & Woosley, S. E. 2000, ApJ, 528, 368
Hjellming, R. M., & Rupen, M. P. 1995, Nature, 375, 464
Höflich, P., Khokhlov, A., & Wang, L. 2001, in 20th Texas Symp. Relativistic Astrophysics, ed. J. C. Wheeler & H. Martel (New York: AIP), 459
Israelian, G., Rebolo, R., Basri, G., Casares, J., & Martin E. L. 1999, Nature, 401, 142
Iwamoto, K., et al. 1998, Nature, 395, 672
Kifonidis, K. 2001, Ph.D. thesis, Max-Planck-Institut für Astrophysik
Kifonidis, K., Plewa, T., Janka, H-Th, & Müller, E. 2000, ApJ, 531, L123
Kippenhahn, R., Ruschenplatt, G., & Thomas, H.-C. 1980, A&A, 91, 175
Lyne, A. G., & Lorimer, D. R. 1994, Nature, 369, 127
MacFadyen, A. I., & Woosley, S. E. 1999, ApJ, 524, 262

MacFadyen, A. I., Woosley, S. E., & Heger A. 2001, ApJ, 550, 410
Maeda, K., Nakamura, T., Nomoto, K., Mazzali, P. A., Patat, F., Hachisu, I. 2002, ApJ, 565, 405
Marietta, E., Burrows, A., & Fryxell, B. 2000, ApJS, 128, 615
Nakamura, T., Umeda, H., Iwamoto, K., Nomoto, K., Hashimoto, M., Hix, R.W., Thielemann, F.-K. 2001, ApJ, 555, 880
Nelemans, G., Tauris, T. M., & van den Heuvel, E. P. J. 1999, A&A, 352, L87
Nomoto, K., et al. 1997, Nucl. Phys. A, 616, 79c
———. 2001a, in Supernovae and Gamma-Ray Bursts, ed. M. Livio et al. (Cambridge: Cambridge Univ. Press), 144
Nomoto, K., Maeda, K., Umeda, H., & Nakamura, T. 2001b, in The Influence of Binaries on Stellar Populations Studies, ed. D. Vanbeveren (Dordrecht: Kluwer), 507
Orosz, J. A., & Bailyn, C. D. 1997, ApJ, 477, 876
Orosz, J. A., et al. 2001, preprint (astro-ph/0103045)
Paczyński, B. 1998, ApJ, 494, L45
Podsiadlowski, Ph., Rappaport, S., & Pfahl, E. 2002, ApJ, 565, 1107
Shahbaz, T., van der Hooft, F., Casares, J., Charles, P. A., & van Paradijs, J. 1999, MNRAS, 306, 89
Spruit, H. C., & Phinney, E. S. 1998, Nature, 393, 139
Strohmayer, T. E. 2001, preprint (astro-ph/0104487)
Thielemann, F.-K., Nomoto, K., & Hashimoto, M. 1996, ApJ, 460, 408
Tingay, S. J., et al. 1995, Nature, 374, 141
van der Hooft, F., Heemskerk, M. H. M., Alberts, F., & van Paradijs, J. 1998, A&A, 329, 538
Umeda, H., & Nomoto, K. 2002, ApJ, 565, 385
Woosley, S. E. 1993, ApJ, 405, 273
Woosley, S. E., & Weaver, T. 1995, ApJS, 101, 181